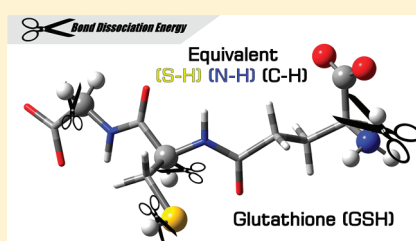


Antioxidant Potential of Glutathione: A Theoretical Study

Béla Fiser,^{†,‡} Milán Szőri,^{†,‡} Balázs Jójárt,^{†,‡} Róbert Izsák,^{‡,§} Imre G. Csizmadia,^{†,‡,||} and Béla Viskolcz^{*,†,‡}[†]Department of Chemical Informatics, Faculty of Education, University of Szeged, Boldogasszony sgt. 6. 6725, Szeged, Hungary[‡]Drug Discovery Research Center, Szeged, Hungary[§]Lehrstuhl für Theoretische Chemie, Institut für Physikalische und Theoretische Chemie, Universität Bonn, Wegelerstrasse 12, 53115 Bonn, Germany^{||}Department of Chemistry, University of Toronto, Toronto, Ontario M5S 3H6, Canada

Supporting Information

ABSTRACT: All possible X–H (where X can be C, N, O or S) bond dissociation energies (BDEs) of glutathione (γ -L-glutamyl-L-cysteinyl-glycine, GSH) and its fragments have been calculated by first principle methods, and the antioxidant potential of GSH was revealed to be higher than expected in earlier studies. Electron delocalization was found to have an important influence on the antioxidant potential. All structures were optimized and their harmonic vibrational frequencies were calculated in the gas phase at the B3LYP/6-31G(d) level of theory. Solvent effects were taken into account for optimizations at the same level of theory by applying the conductor-like polarizable continuum model (CPCM). Hydrogen cleavage from glutathione proved that the G3MP2B3 composite method provides results consistent with the experimental values for bond dissociation enthalpies (ΔH_{298}) of S–H, O–H, C–H, and N–H bonds. In order to replace the G3MP2B3 energies with accurate single point calculations, six density functionals, namely, MPWK CIS, MPWK CIS1K, M06, TPSS1K CIS, TPSSh, and B3LYP, were tested against G3MP2B3 for obtaining accurate bond dissociation energies. The MPWK CIS1K/6-311++G(3df,2p)//B3LYP/6-31G(d) level of theory provides the best correlation with the G3MP2B3 method for BDEs in both phases, and therefore, it is recommended for similar calculations. Gas phase results showed that the O–H bond was the weakest, while in aqueous phase the N–H bond in the ammonium group proved to have the smallest BDE value in the studied system. In both cases, the cleavage of the X–H bond was followed by decarboxylation which was responsible for the energetic preference of these processes over the S–H dissociation, which was regarded as the most favorable one until now. The calculated BDE values showed that in aqueous phase the most preferred H-abstraction site is at the weakest N–H bond ($\text{BDE}_{\text{aq}} = 349.3 \text{ kJ mol}^{-1}$) in the glutamine fragment near the α -carbon. In water, the formation of N-centered radicals compared to S-centered ones ($\text{BDE}_{\text{aq}} = 351.7 \text{ kJ mol}^{-1}$) is more endothermic by 2.54 kJ mol^{-1} , due to decarboxylation. Hydrogen dissociation energies from the α -carbons are also comparable in energy with those of the thiol hydrogen, within computational error. The higher stability of the radicals—except the S-centered ones—is due to various degrees of electron delocalization. In aqueous phase, four quasi-equivalent stable radical centers (the α -carbons, the N-centered radical of the NH_2 group, and the S-centered radical) were found which provide the antioxidant behavior of glutathione.



INTRODUCTION

Radicals play an important role in a number of biological processes (aging, oxidation processes, etc.), without some of which life would be impossible.¹ Moreover, radicals may also be involved in oxidative stress related diseases.^{2,3} Living organisms have developed a number of mechanisms to regulate the amount of radicals^{4,5} to avoid adverse procedures.

A crucial biomolecule in free radical regulation is the linear tripeptide glutathione (γ -L-glutamyl-L-cysteinyl-glycine), denoted as GSH. It is essential in a number of biochemical processes in living organisms, including repair of oxidative damage⁶ and defense of the central nervous system against free radicals.^{7,8} It has also a role in apoptosis, signal transduction, and gene expression.^{9,10} Fluctuating or decreased glutathione concentration leads to neurological diseases, such as Parkinson's or Alzheimer's disease.^{11,12} The glutathione/glutathione disulfide (GSH/GSSG) system is one of the most important intracellular

oxidation–reduction buffers, providing protection against carcinogenic diseases, radical agents of oxidative stress, and lipid peroxidation.^{13–16} Glutathione detoxifies a variety of compounds by forming glutathione conjugates.^{17,18} It also regulates the oxidation state of the SH group in proteins and other biological systems containing thiol groups via homo- and heterodisulfide formation equilibria.¹⁹

GSH can be found in high concentration in the cytosol (1–11 mM), nuclei (3–15 mM), and mitochondria (5–10 mM) of cells;²⁰ furthermore, GSH is the major soluble antioxidant in these cell compartments. The pH dependence of microscopic protonation states of GSH was studied both experimentally²¹ and computationally,²² but the radical-forming ability of these

Received: May 27, 2011

Revised: August 10, 2011

Published: August 18, 2011

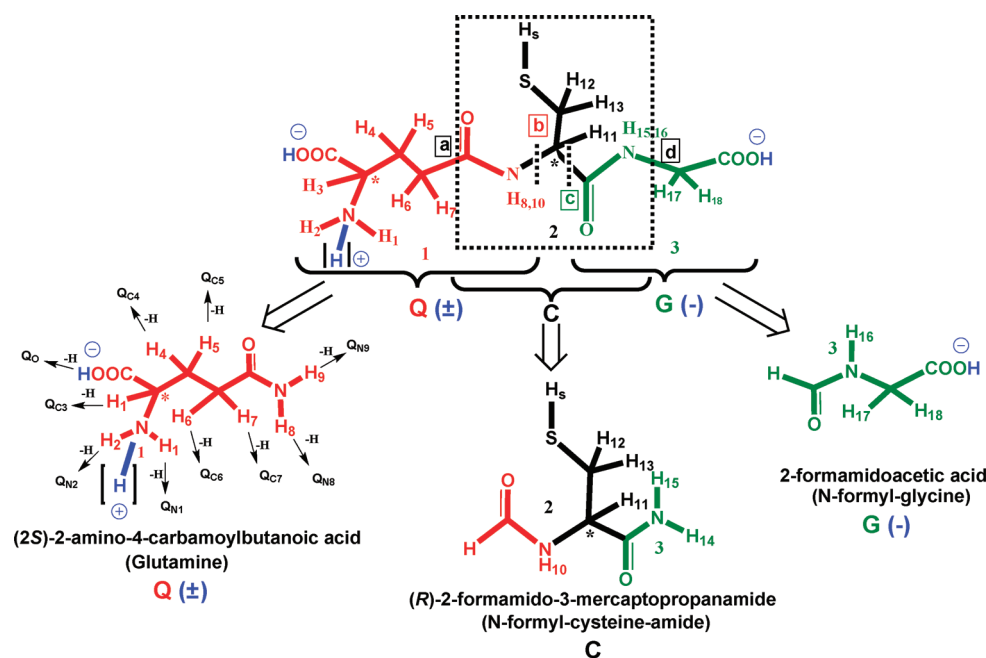


Figure 1. Nomenclature used with glutathione (GSH) and its fragments. Q, C, and G are the overlapping fragments of GSH in the gas phase. In the aqueous phase Q is zwitterionic (protonation on the amine and deprotonation on the carboxyl group, $Q(\pm)$) and G is anionic (deprotonation on the carboxyl group, $G(-)$). The protonation and deprotonation are indicated with blue “+” and “−”, respectively.

solvated states of GSH has not yet been investigated. Experimental conformation analyses have been carried out over the whole pH range.^{23,24} Interestingly, the stability of radicals formed from neutral GSH in the gas phase has been examined extensively,^{25,26} although glutathione anion ($GSH(-)$) is found to be dominant at physiological pH. In the case of $GSH(-)$, L-glutamic acid predominantly exists in its zwitterionic form, while the carboxyl group of the glycine fragment prefers to be deprotonated.²⁷

Herein, we determine the radical-forming ability of the biologically important $GSH(-)$ in a thermodynamic sense. Furthermore, the radical-scavenging ability of GSH and $GSH(-)$ will be compared, and thus the quality of gas phase calculations will be assessed in comparison with results obtained in solution.

METHODOLOGY

In previous attempts, the conformational space of GSH was explored by molecular dynamics simulations, and it was found that GSH is very flexible and does not adopt a strongly preferred conformation at any pH.²² Therefore, the extended structures of GSH are considered in this work. Since accurate and robust quantum chemical calculations are still overly demanding for tripeptides like GSH, a simplification of the whole system (analogous to previous attempts^{28–30}) seems to be necessary. Therefore, the GSH molecule was split into three (overlapping) fragments: (2S)-2-amino-4-carbamoylbutanoic acid (L-glutamine, Q), (R)-2-formamido-3-mercaptopropanamide (N-formyl-L-1-cysteine-amide, C), and 2-formamidoacetic acid (N-formyl-glycine, G). Similar to neutral glutathione, water-soluble ionic $GSH(-)$ can also be partitioned into three pieces: zwitterionic $Q(\pm)$, C, and anionic $G(-)$ (Figure 1). Due to the overlapping fragmentation, L-glutamine (Q) replaces L-glutamic acid (E) in the nomenclature; however, glutathione can be

synthesized from the amino acids L-cysteine (C), L-glutamic acid (E), and glycine (G).

Being a radical scavenger, tripeptide glutathione can function as a hydrogen atom donor. In order to characterize the site preference of radical formation, the X–H (where X can be C, N, O, or S) homolytic bond dissociation energies (BDEs at 0 K) of GSH and the fragments mentioned above were calculated:



where R can be Q, C, or G. The homolytic bond dissociation energy (BDE) can measure the stability of the radicals which are formed from homolytic bond dissociation: it is the energy required to separate the ground state molecule into ground state fragments.³¹ In our case, these fragments are a free radical and a hydrogen atom.

Products of the homolytic X–H bond dissociation reactions are denoted systematically. For instance, Q_{N1} corresponds to the hydrogen at position 1 abstracted from a nitrogen in fragment Q or the equivalent part in the whole GSH (see Figure 1). There are special cases when superscripts are used to separate the different species. For instance, $Q_{N1,2}^{a,b}$ corresponds to the same N–H bond cleavage (and its neighbor) as was detailed above, with the “b” and “a” indicating that after the cleavage of the N–H bond consecutive decarboxylation does or does not occur, respectively. Indices “a” and “b” also refer to the closer and further hydrogens of the protonated amine group from the carboxyl group in fragment Q. BDE values as measures of bond strength are comparable in a range of various chemical species. If BDE values obtained in the same molecule are compared, it is worth using relative BDEs (Δ BDEs), which are analogous to the radical stabilization energy (RSE).³² If the reference reaction is the homolytic dissociation of the S–H bond of GSH (C_S), the hydrogen atom abstraction potentials of the radicals formed can be obtained by calculating the energetic change in the

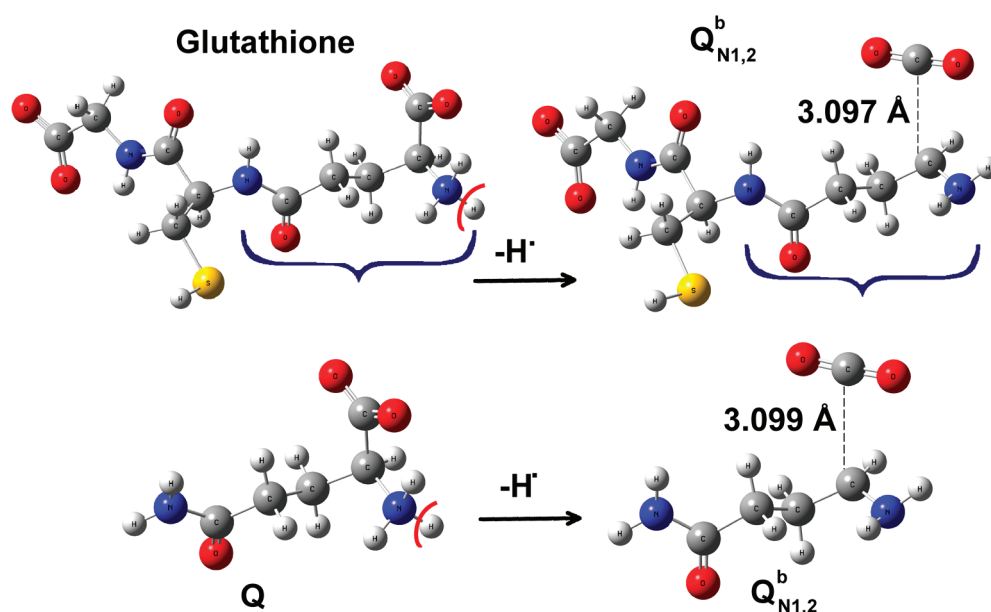


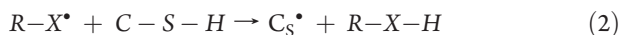
Figure 2. Optimized structures of glutathione and its fragment, with the optimized structure of $Q_{N1,2}^b$ radicals (in the case of the whole system, glutathione) and the fragment in aqueous phase.

Table 1. Comparison of Experimental Bond Dissociation Enthalpies ($DH_{298}(\text{exp})$ in kJ/mol) and Corresponding G3MP2B3 Results of the GSH Species ($DH_{298}(\text{calc})$ in kJ/mol) Obtained at 298 K^a

bond type	phase	compound	experimental		fragment	calculated
			DH_{298} (exp)	ref		DH_{298} (calc)
S–H	water	cysteine (cys-S-H)	353.1	52	C_S	356.2
O–H	gas	CH_3COO-H	468.6 ± 12.6	53	$Q_O (G_O)$	460.9 (483.7)
C–H	gas	$H-CH_2CHO$	394.5 ± 9.2	31	$Q_{C6,7}$	394.9 ± 0.8
N–H	gas	CH_3NH-H	418.4 ± 10.5	54	$Q_{N1,2}^a$	420.9

^aNo consecutive decarboxylation after the cleavage of the X–H bond.

following reaction:



where C_S^\bullet is the S-centered radical in the fragment C. The energetic properties of the X–H bond dissociation determine the antioxidant effect of glutathione. In current literature, the S–H bond is identified as one of the main factors responsible for that effect. Therefore, the BDE of the S–H bond was used as the reference for the calculation of ΔBDE s. A positive ΔBDE indicates that the bond is weaker than the S–H of GSH (C_S).

The G3MP2B3 method can provide accurate thermochemical properties such as heat of formation or BDE³³ for radical systems. This method³⁴ has been chosen as a reference for calculating the BDEs and relative stabilities of the radicals formed from the previously mentioned fragments in gas and aqueous phases (Figure 1). As the first step in the G3MP2B3 procedure, all of these geometry optimizations were carried out using the B3LYP functional³⁵ as implemented in the Gaussian packages^{36,37} with the 6-31G(d) basis set.³⁸ Solvent effects were taken into account in optimizations at the same level of theory by applying the

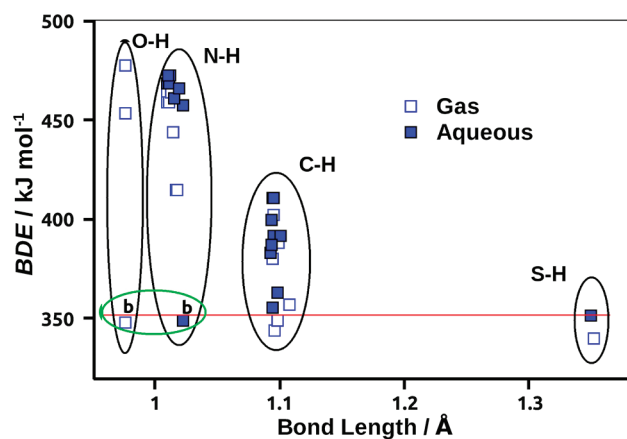


Figure 3. X–H bond dissociation energies (BDE) against bond lengths in gas phase (open squares) and aqueous phase (filled squares). The black ellipses separate the different bond types which belong to different X–H bonds, and the green ellipse includes the consecutive decarboxylations (b).

conductor-like polarizable continuum model (CPCM)^{39,40} (SCRF = CPCM, solvent = water). The solute cavity is built up using radii from the UFF force field, and the standard value of the dielectric constant (ϵ) is employed for water ($\epsilon = 78.3553$). The electrostatic scaling factor (Alpha) for the sphere radius of the atoms was the default value (Alpha = 1.1). Normal mode analysis was carried out on each vacuum and solvent optimized structure at the B3LYP/6-31G(d) level of theory, and calculated harmonic frequencies were scaled by a factor of 0.97⁴¹ to obtain thermochemical properties. To increase the accuracy of results, QCISD(FC,T)/6-31G(d) and MP2(FC)/G3MP2Large single point calculations were also performed as part of the G3MP2B3 procedure.³³

Since the computationally demanding part of the G3MP2B3 method is the calculation of accurate G3MP2 energy, the method

is limited to medium-sized systems, preventing the accurate treatment of a tripeptide (such as GSH). One can overcome

Table 2. G3MP2B3 Bond Dissociation Energies (BDE) (0 K, kJ/mol), Their Relative Values (Δ BDEs) and the Standard Entropies (298.15 K, J/mol·K) in Gas and Aqueous Phases

radical	G3MP2B3					
	BDE		Δ BDE		S	
	gas	aqueous	gas	aqueous	gas	aqueous
C _S	340.3	351.7	0.0	0.0	418.9	425.3
Q _{C3}	357.2	399.9	−16.9	−48.1	460.6	462.3
Q _{C4}	402.5	410.8	−62.2	−59.0	456.2	440.3
Q _{C5}	402.5	410.8	−62.2	−59.0	456.2	440.3
Q _{C6}	389.7	391.9	−49.4	−40.1	451.3	445.9
Q _{C7}	388.2	391.9	−48.0	−40.1	453.1	445.9
C _{C11}	343.9	355.5	−3.6	−3.8	423.0	429.6
C _{C12}	380.4	383.5	−40.1	−31.8	436.0	445.6
C _{C13}	380.4	387.1	−40.1	−35.4	436.0	439.6
G _{C17}	349.3	363.0	−9.0	−11.3	351.0	348.6
G _{C18}	349.3	363.0	−9.0	−11.3	351.0	348.6
Q _{N1,2} ^a	415.0	457.8	−74.7	−106.1	457.0	471.3
Q _{N1,2} ^b	415.0 ^a	349.3 ^b	−74.7 ^a	2.4 ^b	457.0 ^a	528.0 ^b
Q _{N8}	459.4	469.0	−119.1	−117.3	452.6	448.9
Q _{N9}	459.4	469.0	−119.1	−117.3	452.6	448.9
C _{N10}	444.0	461.3	−103.8	−109.5	431.4	432.8
C _{N14}	465.0	473.0	−124.7	−121.3	437.5	437.1
C _{N15}	465.0	473.0	−124.7	−121.3	437.5	437.1
G _{N16}	464.2	466.1	−123.9	−114.4	371.3	364.2
Q _O ^a	453.9	—	−113.6	—	471.2	—
Q _O ^b	348.2	—	−7.9	—	519.6	—
G _O	477.8	—	−137.5	—	368.1	—

^a No consecutive decarboxylation after the cleavage of the X–H bond.

^b Consecutive decarboxylation after the cleavage of the X–H bond.

this issue with the replacement of the G3MP2B3 calculation with an appropriately accurate functional. In order to find such a functional, results of the six metafunctionals MPWKCIS,⁴² MPWKCIS1K,⁴² M06,⁴³ TPSS1KCIS,^{44–46} TPSSh,⁴⁷ and B3LYP, were tested against the G3MP2B3 values. These single point calculations were carried out using the 6-311++G(3df,2p) basis set⁴⁸ on structures obtained at the B3LYP/6-31G(d) level of theory, in both vacuum and solvent. Most of these state-of-the-art hybrid functionals are not directly available in the Gaussian packages; these calculations were carried out using the IOp keyword.⁴² The structural comparisons and the calculation of the root-mean-square-deviation (rmsd) values were carried out using the Molecular Operating Environment (MOE 2010.10).⁴⁹

RESULTS AND DISCUSSION

Geometric Considerations. The glutathione is partitioned and solvent effects can significantly affect BDE values due to structural changes. In order to compare the optimized geometries of the glutathione fragments in gas and aqueous phases (Q and Q(±)_{aq}, C and C_{aq}, G and G(−)_{aq}), the root-mean-square-deviation (rmsd) values of the non-hydrogen atoms have been calculated, respectively. These values are found to be small: the largest rmsd (rmsd_{max}), is less than 0.15 Å and the average (rmsd_{ave}) is 0.09 Å, indicating that there are no significant conformational changes between phases. Actually, the main difference in the above-mentioned structures is due to their protonation states.

In the comparative investigation of the gas and aqueous phase geometries of radicals formed in the hydrogen cleavage of the fragments, the rmsd_{max} value is 1.12 Å and the rmsd_{ave} is less than 0.30 Å. It is evident that the immersion of the GSH fragment radicals into the implicit water model has significant structural effects in some cases. To measure the effect of partitioning glutathione into fragments, structural alignments of the heavy atoms in the fragments to those in GSH were carried out. Such alignments in water showed negligible deviation, as indicated by the corresponding rmsd_{max} and rmsd_{ave} values of 0.07 and 0.05 Å, respectively.

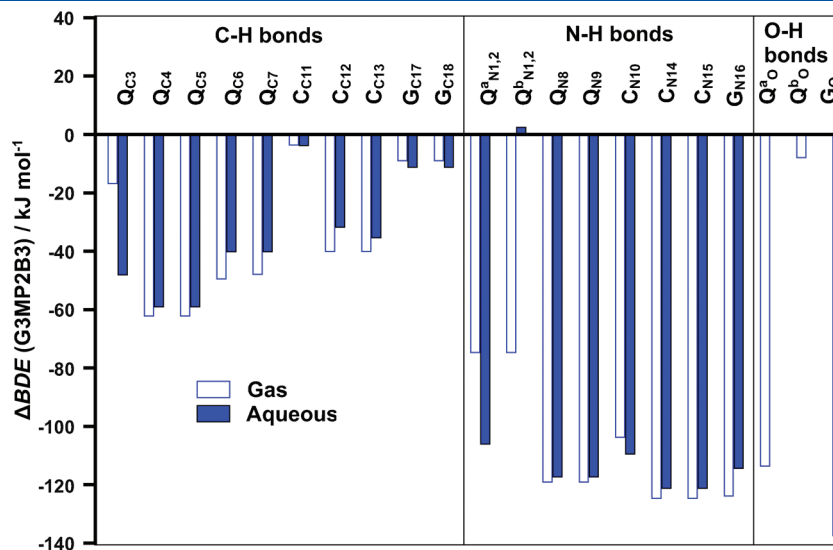


Figure 4. Relative bond dissociation energies (Δ BDEs) in aqueous and gas phases calculated with the G3MP2B3 method. The reference is the BDE of the S–H bond in the fragment C (C_S radical formed by the bond dissociation of S–H).

Table 3. Bond Dissociation Energies (BDE) of the Glutathione Fragments (0 K, kJ/mol) in Gas and Aqueous Phases, Based on B3LYP/6-31G(d) Optimized Geometries (basis set 6-311++G(3df,2p) was selected for all methods)

radical	B3LYP		MPWKICIS		MPWKICIS1K		M06		TPSS1KCIS		TPSSH	
	gas	aqueous	gas	aqueous	gas	aqueous	gas	aqueous	gas	aqueous	gas	aqueous
C _S	329.3	341.6	333.2	345.8	333.9	346.5	334.6	346.5	329.3	342.2	332.8	346.1
Q _{C3}	327.8	376.4	326.3	375.5	338.2	381.5	338.8	382.3	325.1	372.9	330.1	376.7
Q _{C4}	385.7	392.3	385.5	392.8	392.6	397.8	388.9	395.2	381.0	389.2	383.4	392.6
Q _{C5}	385.7	392.3	385.5	392.8	392.6	397.8	388.9	395.2	381.0	389.2	383.4	392.6
Q _{C6}	375.8	374.9	378.1	376.1	382.6	381.4	376.6	376.5	372.5	371.5	376.1	375.3
Q _{C7}	370.8	374.9	372.4	376.1	377.5	381.4	375.5	376.5	367.9	371.5	371.9	375.3
C _{C11}	317.1	329.0	315.2	327.3	328.2	340.1	325.5	335.5	312.3	324.8	316.3	329.1
C _{C12}	364.1	367.3	362.9	366.1	370.0	372.4	367.0	369.9	360.9	364.4	364.6	368.4
C _{C13}	364.1	370.1	362.9	369.0	369.9	375.6	367.0	373.0	360.9	367.1	364.6	371.0
G _{C17}	327.0	343.2	327.0	343.0	337.9	352.2	336.9	351.1	323.8	340.0	328.4	344.4
G _{C18}	327.0	343.2	327.0	343.0	337.9	352.2	336.9	351.1	323.8	340.0	328.4	344.4
Q _{N1,2} ^a	398.8	408.1	404.0	407.1	406.5	439.5	406.9	426.1	391.5	399.7	392.1	401.9
Q _{N1,2} ^{ab}	398.8 ^a	323.1 ^b	404.0 ^a	331.0 ^b	406.5 ^a	346.3 ^b	406.9 ^a	318.0 ^b	391.5 ^a	322.7 ^b	392.1 ^a	330.7 ^b
Q _{N8}	449.7	462.6	455.2	468.6	462.8	474.3	459.6	470.5	442.9	456.1	444.0	457.3
Q _{N9}	449.7	462.6	455.2	468.6	462.8	474.3	459.6	470.5	442.9	456.1	444.0	457.3
C _{N10}	424.5	444.7	426.7	447.1	444.8	464.2	435.0	453.9	415.6	436.0	416.2	436.8
C _{N14}	455.1	466.0	460.9	472.3	468.2	478.2	465.6	475.3	448.0	459.2	449.0	460.5
C _{N15}	455.1	466.0	460.9	472.3	468.2	478.2	465.6	475.3	448.0	459.2	449.0	460.5
G _{N16}	452.7	430.7	458.3	429.5	464.4	462.2	461.9	436.3	446.5	420.8	448.4	422.7
Q _O ^a	430.5	—	430.2	—	459.7	—	452.0	—	419.2	—	419.8	—
Q _O ^b	315.1	—	322.6	—	345.2	—	320.0	—	310.9	—	316.6	—
G _O	440.3	—	439.2	—	472.0	—	463.3	—	427.3	—	427.2	—

^aNo consecutive decarboxylation after cleavage of the X–H bond. ^bConsecutive decarboxylation after cleavage of the X–H bond.

For the radicals, alignment shows somewhat enhanced alteration in the water phase and the rmsd_{ave} value is 0.16 Å. The alignment of gas phase geometries, GSH radicals vs fragment radicals, resulted in a 3 times larger rmsd_{ave} , 0.49 Å. In GSH, there are intramolecular interactions (hydrogen bonds) which have a significant effect on the structure of the glutathione radicals, but these interactions are absent from the fragments. For instance, the hydrogen bonds between the amide nitrogen and the carboxyl oxygen of the two peptide bonds in GSH (typically within the C fragment part) are not present in single fragments. Nevertheless, under biologically relevant conditions, treating glutathione as separated fragments has little influence on geometry.

The largest structural change due to homolytic bond dissociation is found in fragment Q for the Q_O^b radical in the gas phase. The cleavage of the H atom from the carboxyl group (Q_O) can cause a consecutive C–C bond break, resulting in CO₂ dissociation, decarboxylation (Q_O^b), while the oxygen-centered radical species is transformed into a carbon-centered one. This complex phenomenon (H cleavage from carboxyl initiates decarboxylation) has not been observed in the aqueous phase since the carboxyl group is deprotonated in this medium, so there is no O–H bond to be broken. However, the hydrogen from the positively charged amino group can be abstracted in water. This may break the adjacent C–C bond, as indicated by the roughly 2 times greater bond length than that in GSH (see Figure 2).

The largest structural change due to homolytic bond dissociation is found in fragment Q for the Q_{N1,2}^b radical in aqueous phase. This structural realignment also causes a shift of the radical

center from the nitrogen to the carbon. Such cleavage can be interpreted as the breaking N–H bond of the NH₃⁺ group initiating decarboxylation from the formed radical. Actually, this reaction of the Q fragment produces the radical 4-aminobutanamide (which is a protected γ -aminobutyric acid (GABA) radical) and carbon dioxide. Reaction with similar products can also occur naturally via an ionic mechanism by means of glutamate decarboxylase, when glutamate is converted to GABA.⁵⁰

Bond Dissociation Energies of Fragments. The performance of the theoretical models applied can be estimated by direct comparison with experimental data. Bond dissociation enthalpies at 298 K (DH₂₉₈)³¹ were also calculated and compared to experimental data. Bond dissociation enthalpies were used for validation of our calculations, and the collected results are shown in Table 1.

In the case of the S–H bond, the G3MP2B3 method reproduces the experimental bond dissociation enthalpy measured in the aqueous phase within chemical accuracy. The calculated BDE values of the C–H and N–H bonds are in good agreement with the experimental ones in the gas phase. Although the deviation is more enhanced for the O–H bond in the gas phase, it is still moderate and probably arises from the absence of the primary amine groups in the measured structure (acetic acid), which are close to the O–H bonds in the fragments. It is also important to point out that the standard deviation of the gas phase experimental values is also very large for both cases (10 kJ/mol). Therefore, it was concluded that the G3MP2B3 model chemistry is able to provide reasonable bond dissociation enthalpies for glutathione fragments.

The analysis of BDE values calculated with the G3MP2B3 method shows that there are distinguishable geometric classes corresponding to the bond lengths of the X–H bonds, where X can be C, N, O, and S. These classes are also separated by the appropriate BDE range (see Figure 3). The data collected in Table 2 show that the BDE values of the C–H bonds can vary from 343 to 403 kJ/mol in the gas phase. The hydrogen atoms bonded to the α -carbons (Q_{C3} , C_{C11} , G_{C17} , and G_{C18}) were found to be the most weakly bound among the C–H bonds with BDEs from 343.9 to 357.2 kJ/mol. The aqueous medium makes these bonds stronger by 11–42.9 kJ/mol. The medium has the largest influence (42.9 kJ/mol) on C–H BDE in the case of glutamine α -carbon (Q_{C3}). This may be due to the zwitterionic structure of glutamine.⁵¹ The N–H bonds in the aqueous form of glutathione are stronger, though, as indicated by the corresponding gas phase BDE values (415–465 kJ/mol). The O–H bonds are in the same BDE range as the N–H ones. Although the S–H bond is known to be the weakest, Figures 3 and 4 clearly demonstrate that S–H, C–H, N–H, and O–H can have quite similar BDEs in some cases. The Δ BDE values are used to measure the relative strength of X–H bonds compared to that of the S–H bond in glutathione and its fragments.

As Figure 4 shows, the Δ BDEs for C_{C11} , G_{C17} , G_{C18} , and Q_{C3} are only around 10 kJ/mol stronger than that for the S–H bond. These hydrogens connected to α -carbons constitute the weakest bonds in the gas phase. The weakest one corresponds to C_{C11} , with Δ BDE = –3.6 kJ/mol compared to the S–H bond. It is clear from Table 2 that the O–H bond (Q_O^b) dissociation energy is one of the smallest in the gas phase, with its slightly negative Δ BDE (–7.9 kJ/mol) being comparable with that for the α -C–H bonds, making this O–H also somewhat harder to break than the S–H bond in the gas phase.

The BDE value of Q_{C3} increases in the aqueous phase and becomes comparable with that of the non- α -C–H bonds. The corresponding Δ BDE is –48.1 kJ/mol, which is smaller than any relative C–H bond dissociation energy except those of Q_{C4} and Q_{C5} (Δ BDE = –59.0 kJ/mol). This means that Q_{C3} is the strongest C–H bond in the aqueous phase after the β -C–H bonds ($Q_{C4,5}$) of fragment Q. This change in the BDE value can be attributed to the steric effects of the nearby protonated amine group.

The C–H bonds of the α -carbons in fragments G ($G_{C17,C18}$) and C (C_{C11}) are as weak as the thiol bond is in the aqueous phase. The deviation between the S–H and C–H BDE values for $G_{C17,C18}$ is only 11 kJ/mol. Furthermore, the hydrogen abstraction from the α -carbon in fragment C is more preferable than from G. This bond (C_{C11}) is only 3.8 kJ/mol stronger than the S–H bond. Nevertheless, the N–H bond belonging to $Q_{N1,2}^b$ is 2.4 kJ/mol weaker than the S–H bond, and this is the weakest bond due to the consecutive decarboxylation from the radical after the hydrogen atom cleavage in the aqueous phase. These can be immediately seen from Figure 4, and such results raise doubts about the established view on S–H and α -C–H hegemony in the antioxidant properties of glutathione. The maximal entropy belongs to Q_O^b in the gas phase and to $Q_{N1,2}^b$ in the aqueous phase (see the last two columns in Table 2). This indicates that the entropy contribution to the Gibbs free energy of the bond dissociation might further increase the preference of the cleavage of the hydrogen over breaking the S–H bond.

Comparing gas and aqueous phase Δ BDE values, no dramatic difference was found (all were less than 10 kJ/mol) except in the cases where large structural changes were recognized. The case of

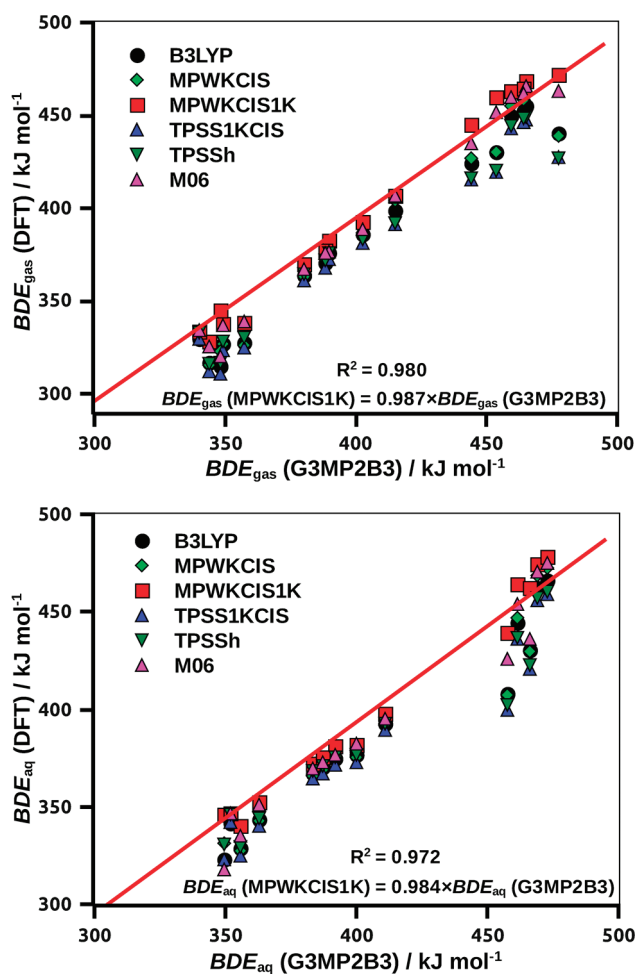


Figure 5. Comparisons of bond dissociation energies (BDEs) obtained using several density functionals to those of the G3MP2B3 method, calculated in gas (top) and aqueous (bottom) phases. MPWKIS1K provides the best fit to G3MP2B3, in both the gas and aqueous phases. Coefficients for the lines of the best fit are also given.

O–H bonds were excluded, since carboxyl groups are deprotonated in the aqueous phase, so O–H bond dissociation is not possible. Q_{C3} shows moderate change (31.2 kJ/mol) by alteration of the surrounding medium. Δ BDE values of $Q_{N1,2}^b$ in gas and aqueous phases differ by as much as 77.1 kJ/mol. This is the largest difference between the gas and aqueous phase Δ BDE values.

In order to calculate the bond dissociation properties for glutathione as a whole, a density functional has to be selected with the capacity of reproducing the G3MP2B3 results. Accordingly, the bond dissociation energies are recalculated using B3LYP, MPWKIS, MPWKIS1K, M06, TPSS1KCIS, and TPSSh functionals with the 6-311++G(3df,2p) basis set on B3LYP/6-31G(d) geometries (see Table 3) for both media. Figure 5 shows the calculated bond dissociation energies obtained from different density functional computations against those of G3MP2B3 in the gas phase (top panel) and in the aqueous phase (bottom panel). These graphs include the best linear fits, and the corresponding equations are also given. In both media, the G3MP2B3 BDE values are best approximated by MPWKIS1K/6-311++G(3df,2p)//B3LYP/6-31G(d) calculations out of the B3LYP, MPWKIS, MPWKIS1K, M06, TPSS1KCIS,

Table 4. BDEs and Relative BDEs in the Case of the Whole Glutathione, Calculated by B3LYP and MPWKIS1K Functionals in Gas and Aqueous Phases (0 K, kJ/mol), Based on B3LYP/6-31G(d) Optimized Geometries

radical	B3LYP/6-31G(d)				MPWKIS1K/6-311++G(3df,2p)			
	BDE		Δ BDE		BDE		Δ BDE	
	gas	aqueous	gas	aqueous	gas	aqueous	gas	aqueous
C _S	335.6	336.5	0.0	0.0	351.3	349.1	0.0	0.0
Q _{C3}	335.3	380.5	0.4	−43.9	338.7	381.6	12.7	−32.5
Q _{C4}	379.5	396.8	−43.9	−60.2	387.5	399.2	−36.2	−50.1
Q _{C5}	381.8	396.5	−46.1	−60.0	389.5	398.8	−38.2	−49.7
Q _{C6}	377.2	375.9	−41.6	−39.4	381.7	379.7	−30.4	−30.6
Q _{C7}	372.2	375.9	−36.6	−39.4	374.9	379.7	−23.5	−30.6
C _{C11}	347.5	331.3	−11.9	5.3	355.6	342.6	−4.3	6.5
C _{C12}	377.5	379.1	−41.8	−42.5	374.1	372.9	−22.8	−23.7
C _{C13}	377.5	379.5	−41.8	−42.9	374.1	376.4	−22.8	−27.3
G _{C17}	326.1	350.9	9.5	−14.4	334.7	354.2	16.6	−5.1
G _{C18}	326.1	350.9	9.5	−14.4	334.7	354.2	16.6	−5.1
Q _{N1,2} ^a	403.6	394.1	−68.0	−57.5	421.6	440.1	−70.3	−91.0
Q _{N1,2} ^{a,b}	391.3 ^a	321.6 ^b	−55.7 ^a	14.9 ^b	408.9 ^a	346.6 ^b	−57.6 ^a	2.5 ^b
Q _{N8,9}	415.7	421.6	−80.0	−85.0	443.1	456.6	−91.8	−107.5
C _{N10}	415.7	421.6	−80.0	−85.0	443.1	456.6	−91.8	−107.5
C _{N14,15}	437.2	395.8	−101.6	−59.2	452.7	453.4	−101.3	−104.3
G _{N16}	437.2	395.8	−101.6	−59.2	452.7	453.4	−101.3	−104.3
Q _O ^a	414.8	—	−79.1	—	461.5	—	−110.1	—
Q _O ^b	318.2	—	17.5	—	344.1	—	7.3	—
G _O	412.6	—	−77.0	—	462.2	—	−110.8	—

^a No consecutive decarboxylation after cleavage of the X–H bond. ^b Consecutive decarboxylation after cleavage of the X–H bond.

and TPSSh results. In the gas phase, the linear fit between MPWKIS1K and G3MP2B3 values is almost perfect (slope = 0.987 and $R^2 = 0.980$). The fit is somewhat less good for aqueous results (slope is 0.984 and $R^2 = 0.972$), but still acceptable. Interestingly, those strong N–H bonds which have a BDE greater than 450 kJ/mol proved hard to calculate with most density functionals tested here in either phase. It is worth pointing out that M06 also provides better correlation with G3MP2B3 than B3LYP, MPWKIS, TPSS1KCIS, and TPSSh. However, MPWKIS1K yields slightly better overall results than M06. The selected MPWKIS1K functional has a much smaller computational demand than G3MP2B3, and it is likely to give the most accurate results for GSH.

Radical Scavenging Potential of Glutathione. Experience obtained from the study of glutathione fragments needs to be extended to the glutathione species. For this reason, the bond dissociation energies were calculated using the selected density functional, MPWKIS1K, in both phases. These results are summarized in Table 4. It was found that energy values obtained for fragments are consistent with those calculated for the entire glutathione.

In the gas phase there are four bonds (where H is connected to the α -carbons (Q_{C3}, G_{C17}, G_{C18}) and the carboxyl oxygen (Q_O^b) weaker than S–H mainly due to electron delocalization (see Figure 6). Q_{C3} and G_{C17,18} (Δ BDE = 12.7 and 16.6 kJ/mol, respectively) are weaker than the C_S bond. Only the C_{C11} (the α -carbon–H in fragment C) is somewhat stronger than the S–H bond (Δ BDE = −4.3 kJ/mol). Furthermore, the gas phase relative bond dissociation energy for the O–H bond in fragment

Q is 7.3 kJ/mol, which makes this also more preferable than S–H (because of decarboxylation).

The aqueous phase results for glutathione and its radical species follow the trend observed for the fragments. The BDE values increase due to the structural influence of the aqueous medium. There are three preferred positions (the thionyl group and the α -carbons) to lose an H-atom while GSH transforms into different types of radicals. The thionyl group (S–H bond) itself is rather weak and needs no conjugation to have a small energy difference between GSH and its sulfur-centered radical (C_S). In contrast, the cleavage of the bonds between α -carbons and H-atoms (C_{C11}, G_{C17,C18}) allows for delocalized electrons stabilizing the radical product. These radicals are similar to each other, and the number of electrons involved in the delocalization is proportional to the stability of the conjugated species.

The Q_{N1,2}^b position is also preferred, but this radical dissociates immediately. The fast rearrangement of the electron system results in an unsaturated carbon-centered radical (for fragments, the 4-aminobutanamide radical is produced; for GSH, the product is the decarboxylated glutathione (dGSH) radical) (see Figure 2).

The bond strength of Q_{C3} changes (with a 45 kJ/mol change in BDE) in the same way as in the case of the fragments, and in water the S–H bond is preferable (Δ BDE = −32.5 kJ/mol). The BDE of G_{C17,18} is also high, but not as much as in the case of the α -carbon–H bond in fragment Q. It remains comparable with the bond dissociation energy of C_S.

The BDE of the α -C–H in fragment C decreased, and the breaking of fragment Q's N–H bond in the NH₃⁺ group initiates

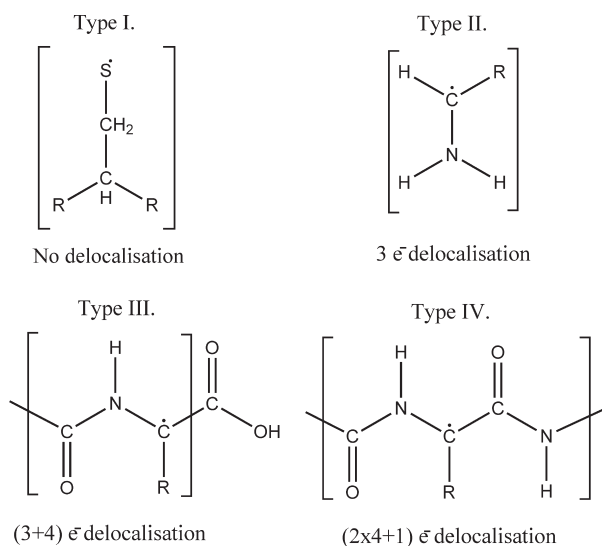


Figure 6. GSH radicals classified into four types based on electron delocalization. There are zero, three, seven, and nine delocalized electrons in the S-centered (C_S), C-centered ($Q_{N1,2}^b$), and α -carbon-centered radicals ($G_{C17,C18}$ and C_{C11}), respectively.

the decarboxylation from the formed radical in the aqueous phase (see Figure 2). Thus, $Q_{N1,2}^b$ and C_{C11} are weaker and hydrogen cleavages are more preferred from here than from the S–H bond ($\Delta BDE = 2.5$ and 6.5 kJ/mol, respectively) under biologically relevant conditions.

The geometric and energetic behavior of the GSH radicals and the glutathione fragment radicals shows that electron delocalization is one of the most important factors of radical stability. In the aqueous phase four particularly important electron delocalization types were found for the radicals (see Figure 6).

As opposed to earlier views which assumed the dominance of S–H and α -C–H bonds in the antioxidant properties of glutathione, it turns out that there are several almost energetically equivalent sites to form radicals. The description suggested here for the GSH system seems to be more complex than what was previously thought. We hypothesize that the effectiveness of glutathione as a water-soluble radical scavenger is likely due to its multiple radicalization sites. The formed radicals have the ability to transform rapidly into one another as dictated by the environment.

CONCLUSIONS

Bond dissociation energies, BDEs, have been calculated in both gas and aqueous phases for all X–H bonds (where X can be C, N, O, and S) of glutathione, and their values have been compared. According to our results, the O–H bond dissociation of the carboxyl group has the smallest bond dissociation energy in a vacuum. In the aqueous phase, the weakest X–H bond is the N–H bond of the glutamine residue ($Q_{N1,2}^b$) in the vicinity of the negatively charged carboxyl group. In both cases, CO₂ formation (decarboxylation) can accompany the breaking of the X–H bond, making the dissociation energetically more favorable than the cleavage of the S–H bond. The N–H bond is stronger than the C–H bond in the gas phase, but protonation significantly weakens it. Furthermore, C–H bonds with α -carbons are found to be about as weak as the sulfhydryl bond of the cysteine residues. Electron delocalization was found to have an important

influence on the antioxidant potential. As clearly evident from our results, glutathione has five possible positions to scavenge a free radical in biologically relevant conditions.

From a methodological perspective, the study of these hydrogen cleavages from glutathione has proven that the G3MP2B3 composite method provides results consistent with the experimental values. In order to replace the G3MP2 energy with accurate single point calculations, six density functionals, namely, MPWKICIS, MPWKICIS1K, M06, TPSS1KCIS, TPSSh, and B3LYP, have been tested against G3MP2 for obtaining accurate bond dissociation energies. These single point calculations were carried out on the fragment structures obtained at the B3LYP/6-31G(d) level of theory in both vacuum and solvent. The MPWKICIS1K/6-311++G(3df,2p)//B3LYP/6-31G(d) level of theory provides the best correlation with the G3MP2B3 method for BDE in both phases, and therefore, this method is recommended for similar calculations.

ASSOCIATED CONTENT

S Supporting Information. Optimized geometries, unscaled frequencies and rotational constants, thermal corrections, and single point energies (B3LYP, MPWKICIS, MPWKICIS1K, M06, TPSS1KCIS, TPSSh) for all compounds. This material is available free of charge via the Internet at <http://pubs.acs.org>.

AUTHOR INFORMATION

Corresponding Author

*E-mail: viskolcz@jgypk.u-szeged.hu. Web: www.drugcent.com.

ACKNOWLEDGMENT

The authors thank M. Labádi and L. Müller for the administration of the computer clusters used for this work. We also thank M. Sourisseau for the fruitful discussion. This work was supported by the project "TÁMOP-4.2.1/B-09/1/KONV-2010-0005—Creating the Center of Excellence at the University of Szeged", which is supported by the European Union and cofinanced by the European Regional Fund.

REFERENCES

- (1) Gutteridge, J. M. C.; Halliwell, B. *Ann. N.Y. Acad. Sci.* **2000**, 899, 136–147.
- (2) Harman, D. *Age* **1995**, 18, 97–119.
- (3) Koutsilieri, E.; Scheller, C.; Grünblatt, E.; Nara, K.; Li, J.; Riederer, P. *J. Neurol.* **2002**, 249 (Suppl 2), II/1–II/5.
- (4) Yasui, K.; Baba, A. *Inflammation Res.* **2006**, 55, 359–363.
- (5) Meister, A. *J. Biol. Chem.* **1994**, 269, 9397–9400.
- (6) Axelsson, K.; Mannervik, B. *FEBS Lett.* **1983**, 152, 114–118.
- (7) Chatterjee, S.; Noack, H.; Possel, H.; Keilhoff, G.; Wolf, G. *Glia* **1999**, 27, 152–161.
- (8) Dringen, R.; Kussmaul, L.; Gutterer, J. M.; Hirrlinger, J.; Hamprecht, B. *J. Neurochem.* **1999**, 72, 2523–2530.
- (9) Arrigo, A. P. *Free Radical Biol. Med.* **1999**, 27, 936–944.
- (10) Voehringer, D. *Free Radical Biol. Med.* **1999**, 27, 945–950.
- (11) Monte, D. A. D.; Chan, P.; Sandy, M. S. *Ann. Neurol.* **1992**, 32 (Suppl), S111–S115.
- (12) Schulz, J. B.; Lindenau, J.; Seyfried, J.; Dichgans, J. *Eur. J. Biochem.* **2001**, 267, 4904–4911.
- (13) Pocernich, C. B.; Cardin, A. L.; Racine, C. L.; Lauderback, C. M.; Butterfield, D. A. *Neurochem. Int.* **2001**, 39, 141–149.

- (14) Andrada, M. F.; Martínez, J. C. G.; Szori, M.; Zamarbide, G. N.; Vert, F. T.; Viskolcz, B.; Estrada, M. R.; Csizmadia, I. G. *J. Phys. Org. Chem.* **2008**, *21*, 1048–1058.
- (15) Chakravarthi, S.; Jessop, C. E.; Bulleid, N. J. *EMBO Rep.* **2006**, *271*–275.
- (16) Spector, A. J. *Ocul. Pharmacol. Ther.* **2000**, *16*, 193–201.
- (17) Dixon, D. P.; Laphorn, A.; Edwards, R. *Genome Biol.* **2002**, *3*, 3004.1–3004.10.
- (18) Izsak, R.; Jojart, B.; Csizmadia, I. G.; Viskolcz, B. *J. Chem. Inf. Model.* **2006**, *46*, 2527–2536.
- (19) Ghezzi, P. *Free Radical Res.* **2005**, *39*, 573–580.
- (20) Schafer, F. Q.; Buettner, G. R. *Free Radical Biol. Med.* **2001**, *30*, 1191–1212.
- (21) Noszál, B.; Szakács, Z. *J. Phys. Chem. B* **2003**, *107*, 5074–5080.
- (22) Lampela, O.; Juffer, A. H.; Rauk, A. *J. Phys. Chem. A* **2003**, *107*, 9208–9220.
- (23) York, M. J.; Beilharz, G. R.; Kuchel, P. W. *Int. J. Pept. Protein Res.* **1987**, *29*, 638–646.
- (24) Fujiwara, S.; Formicka-Kozłowska, G.; Kozłowski, H. *Bull. Chem. Soc. Jpn.* **1977**, *50*, 3131–3135.
- (25) Abedinzadeh, Z.; Gardés-Albert, M.; Ferradini, C. *Int. J. Radiat. Appl. Instrum., C* **1992**, *40*, 551–558.
- (26) Sjöberg, L.; Eriksen, T. E.; Révész, L. *Radiat. Res.* **1982**, *89*, 255–263.
- (27) Han, Y.; HaoMiao, Z.; Jian, S. *Sci. China Ser. B* **2007**, *50*, 660–664.
- (28) Ding, V. Z. Y.; Dawson, S. H. S.; Lau, W. Y. L.; Lee, D. R.; Galant, N. J.; Setiadi, D. H.; Jójárt, B.; Szóri, M.; Mucsi, Z.; Viskolcz, B.; Jensen, S. J. K.; Csizmadia, I. G. *Chem. Phys. Lett.* **2011**, *507*, 168–173.
- (29) Galant, N. J.; Wang, H.; Lee, D. R.; Mucsi, Z.; Setiadi, D. H.; Viskolcz, B.; Csizmadia, I. G. *J. Phys. Chem. A* **2009**, *114*, 9138–9149.
- (30) Sahai, M. A.; Viskolcz, B.; Pai, E. F.; Csizmadia, I. G. *J. Phys. Chem. B* **2007**, *111*, 11592–11602.
- (31) Berkowitz, J.; Ellison, G. B.; Gutman, D. *J. Phys. Chem.* **1994**, *98*, 2744–2765.
- (32) Wood, G. P. F.; Moran, D.; Jacob, R.; Radom, L. *J. Phys. Chem. A* **2005**, *109*, 6318–6325.
- (33) Janoschek, R.; Rossi, M. J. *Int. J. Chem. Kinet.* **2002**, *34*, 550–560.
- (34) Baboul, A. G.; Curtiss, L. A.; Redfern, P. C.; Raghavachari, K. *J. Chem. Phys.* **1999**, *110*, 7650–7657.
- (35) Becke, A. D. *J. Chem. Phys.* **1993**, *98*, 1372–1377.
- (36) Frisch, M. J.; Trucks, G. W.; Schlegel, H. B.; Scuseria, G. E.; Robb, M. A.; Cheeseman, J. R.; Montgomery, J. A., Jr.; Vreven, T.; Kudin, K. N.; Burant, J. C.; et al. *Gaussian 03*, revision C.02; Gaussian, Inc.: Wallingford, CT, USA, 2004.
- (37) Frisch, M. J.; Trucks, G. W.; Schlegel, H. B.; Scuseria, G. E.; Robb, M. A.; Cheeseman, J. R.; Scalmani, G.; Barone, V.; Mennucci, B.; Petersson, G. A.; et al. *Gaussian 09*, revision A.1; Gaussian, Inc.: Wallingford, CT, USA, 2009.
- (38) Petersson, G. A.; Bennett, A.; Tensfeldt, T. G.; Al-Laham, M. A.; Shirley, W. A.; Mantzaris, J. *J. Chem. Phys.* **1988**, *89*, 2193–2218.
- (39) Barone, V.; Cossi, M. *J. Phys. Chem.* **1998**, *102*, 1995–2001.
- (40) Cossi, M.; Rega, N.; Scalmani, G.; Barone, V. *J. Comput. Chem.* **2003**, *24*, 669–681.
- (41) Sinha, P.; Boesch, S. E.; Gu, C.; Wheeler, R. A.; Wilson, A. K. *J. Phys. Chem. A* **2004**, *108*, 9213–9217.
- (42) Zhao, Y.; González-García, N.; Truhlar, D. G. *J. Phys. Chem. A* **2005**, *109*, 2012–2018.
- (43) Zhao, Y.; Truhlar, D. G. *Theor. Chem. Acc.* **2008**, *120*, 215–241.
- (44) Krieger, J. B.; Chen, J.; Iafrate, G. J.; Savin, A. In *Electron Correlations and Materials Properties*; Plenum: New York, 1999; pp 463–477.
- (45) Tao, J.; Perdew, J. P.; Staroverov, V. N.; Scuseria, G. E. *Phys. Rev. Lett.* **2003**, *91*, 146401-1–146401-4.
- (46) Zhao, Y.; Truhlar, D. G. *J. Phys. Chem. Chem. Phys.* **2005**, *7*, 2701–2705.
- (47) Staroverov, V. N.; Scuseria, G. E.; Tao, J.; Perdew, J. P. *J. Chem. Phys.* **2003**, *119*, 12129–12137.
- (48) Frisch, M. J.; Pople, J. A.; Binkley, J. S. *J. Chem. Phys.* **1984**, *80*, 3265–3269.
- (49) Molecular Operating Environment (MOE); Chemical Computing Group, Inc., Montreal, Quebec, Canada, 2010.
- (50) Bao, J.; Cheung, W. Y.; Wu, J.-Y. *J. Biol. Chem.* **1995**, *270*, 6464–6467.
- (51) Hofstetter, D.; Nauser, T.; Koppenol, W. H. *Chem. Res. Toxicol.* **2010**, *23*, 1596–1600.
- (52) Warren, J. J.; Tronic, T. A.; Mayer, J. M. *Chem. Rev.* **2010**, *110*, 6961–7001.
- (53) Blanksby, S. J.; Ellison, G. B. *Acc. Chem. Res.* **2003**, *36*, 255–263.
- (54) Sunderlin, L. S.; Panu, D.; Puranik, D. B.; Ashe, A. J.; Squires, R. R. *Organometallics* **1994**, *13*, 4732–4740.